

Note: Even numbered pages are missing

High Energy Facilities  
Accelerator Development Branch  
BROOKHAVEN NATIONAL LABORATORY  
Associated Universities, Inc.  
Upton, New York 11973

SSC Technical Note No. 38  
SSC-N- 82

Results from Heater-Induced Quenches of a 4.5 m Two-In-One  
Superconducting R&D Dipole for the SSC

G. Ganetis and A. Prodell

November 5, 1985

High Energy Facilities  
Accelerator Development Branch  
BROOKHAVEN NATIONAL LABORATORY  
Associated Universities, Inc.  
Upton, New York 11973

SSC Technical Note No. 38  
(SSC-N-82)

Results from Heater-Induced Quenches of a 4.5 m Two-In-One  
Superconducting R&D Dipole for the SSC

G. Ganetis and A. Prodell

November 5, 1985

Abstract

Quench studies were performed using a 4.5 m long SSC R&D dipole to determine the temperature rise during a quench by measuring the resistance of the conductor cable in the immediate vicinity of the quench. The 2-in-1 magnet was wound with improved "high homogeneity" NbTi conductor in a 2-layer cosine  $\theta$  coil configuration of 3.2 cm inner diameter with each layer powered separately to simulate graded conductor. Twelve pairs of voltage taps were installed at various locations in the coils around one bore of the magnet. "Spot" heaters were placed between the voltage taps of 8 of these pairs to initiate magnet quenches. The resistance of the conductor was obtained from observations of the current and voltage during a magnet quench. The temperature of the conductor was then determined by comparing its resistance to an R vs T curve measured independently for the conductor. The quantity  $\int I^2 dt$  is presented as a function of current and location, and the maximum conductor temperature is shown as a function of  $\int I^2 dt$  and location. Measured longitudinal and azimuthal quench propagation velocities are also presented.

---

\*Work performed under the auspices of the U.S. Department of Energy.

heaters positioned on the straight sections of the coils. These pairs of taps, which are designated in Fig. 1 by the numbers 5 and 6 on each coil, were used to determine the azimuthal quench velocity. The leads from each pair of voltage taps were carefully twisted to minimize any induced voltage in the voltage tap signal due to a change in magnetic field.

Table I. Conductor Parameters for the SSC R&D Dipole

Multifilamentary Wire

Superconductor	Nb 46.5 wt % Ti High Homogeneity Alloy
Diameter	.681 mm
Filament Diameter	19 microns
No. of Filaments	528
Cu to SC Ratio	1.3 to 1

Cabled Conductor

Width (bare)	7.823 mm
Mean Thickness (bare)	1.257 mm
Keystone Angle	2.8°
No. of Wires	23
Filling Factor	88%
Insulation Thickness	
Kapton	0.0508 mm
Fiberglass-epoxy	0.0762 mm

Experimental Results

Since one of the objectives of the tests was to measure the highest temperature to which the conductor could be raised before the magnet was damaged, the first heater quenches were made at a constant bath temperature of 4.4°K at different values of magnet current to determine the current,  $I_m$ , at which  $\int I^2 dt$  was

and thus the resistance increase rapidly as the quench propagates away from the heater toward the voltage taps as both  $\rho$  and  $l$  are increasing in the relationship,  $R = \rho l/A$ . The slope changes when the normal quench fronts reach the voltage taps since  $l$  is now constant between the taps and  $R$  is a function only of  $\rho$ . From such traces, for each heater quench the time from the beginning of the quench to the time when the entire 12.7 cm length is resistive can be measured. Half this time multiplied by  $I^2$  gives  $\Delta \int I^2 dt$ , the difference in  $\int I^2 dt$  between the hot spot and the length of 6.35 cm which, to first approximation, is the position corresponding to  $T_{ave}$ .  $R$  is then corrected by adding  $\Delta R$  where  $\Delta R = \Delta \int I^2 dt / d(\int I^2 dt) / dR$  and with this addition the hot spot temperature is found. The corrections for these tests varied from less than  $1^\circ K$  to  $15^\circ K$ .

The curves in Fig. 4 show the temperature rise of the section of conductor where a heater quench was initiated as a function of  $\int I^2 dt$  for locations OMPL and OEL. The curves for the inner coil, IMPL and IEL, not shown, followed closely the curve for OMPL to a maximum of  $345^\circ K$  for IEL and  $280^\circ K$  for IMPL. As mentioned above, the current in the outer coil (curves OMPL and OEL) was 35% greater than that in the inner coil. It was apparent from Fig. 2 that larger values of  $\int I^2 dt$  for a given current could be obtained during a heater quench by firing the heater (OEL) near the end of the outer coil. This heater was then used in the final series of heater quenches at reduced liquid He bath temperatures in an attempt to damage the magnet coil. After each heater quench in this series the magnet current was increased until a quench occurred to ascertain if there had been any deterioration in the magnet performance. For the last heater quench which caused no damage,  $\int I^2 dt = 8.72$  MIITS and  $T = 920^\circ K$ . For the next and last heater quench which damaged the magnet,  $\int I^2 dt = 9.04$  MIITS and  $T$  reached an estimated  $1170^\circ K$ . The He bath temperature for these last quenches was  $2.4^\circ K$ .

$$\beta = dj_{sc}/dT$$

$$i_q = \text{quench current density}$$

and

$$v_a = \frac{i}{C_p} \left\{ \frac{\rho_0 k_a (1-\alpha) \beta}{R \alpha (i_q - i)} \right\}^{1/2} \sim C'_a \frac{i}{(i_q - i)^{1/2}}$$

where:

$$k_a = \text{effective azimuthal conductivity}$$

$$R = \text{resistance ratio}$$

By appropriate substitution, the above relationship for  $T_{\max}$  can also be written:

$$T_{\max} = A \left\{ \frac{E_m i^4 (i_q - i)^{2/5}}{\alpha^{1.5} (1-\alpha) i_q^2} \right\}$$

For a given conductor at a constant He bath temperature:

$$T_{\max} = A' \left\{ \frac{i^4 (i_q - i)^{2/5}}{i_q^2} \right\}$$

If the bath temperature is decreased,  $i_q$  and  $E_m = 1/2 Li_q^2$  increase. For the outer coil of this magnet,  $T_{\max}$  was achieved at  $i = 0.76 i_q$ . Substituting in the expression above for  $E_m$  and  $i_q$ , the expression:

$$T_{\max} = A'' (0.63 i^2) \text{ is obtained.}$$

In the following an attempt is made to compare the functional dependence of temperature and velocities given in the relationships above with the measured values of these quantities.

heater #4 produced similar results, the quench front reaching locations 8 and 7 before any decrease in magnet current was observed but reaching location 3 only after the magnet current had decayed by up to 25 percent. No current decay was observed when the heaters located at 4 on the inner and outer coils were used to determine the azimuthal quench velocities as the quench front propagated to locations marked 6.

Figure 14 shows the developing temperature profile in the magnet after a heater-induced quench has been initiated. The numbers at each curve indicate the locations (see Fig. 2) where the temperature is calculated. Figures 15 and 16 show the temperature profiles for the magnet after quenches have been initiated at OMPL and OEL respectively from the time the quenches started until after the maximum temperatures have been reached in the magnet conductor.

Figure 17 illustrates a plot of  $T_m \propto A'' (0.63 I^2)$  as a function of  $I$  where this dependence on  $I$  is obtained by setting  $I = 0.76 I_q$  the value of  $I$  at which experimentally,  $\int I^2 dt$  is a maximum at any given He bath temperature. The shape of this curve is compared with those obtained experimentally for  $T_m$  as a function of  $I$  for OMPL and OEL.

The relationship

$$T_{\max} = T_0 \left\{ \frac{15 EI^4}{w_0^2 v_l v_a f_0^3 \alpha^2} \right\}^{2/5}$$

was used to calculate  $T_{\max}$  at OMPL and OEL at a magnet current,  $I$ , of 4.5 kA and a helium bath temperature of 4.5°K. Measured values of  $v_l$  and  $v_a$  were used in the calculations. The calculated value for OMPL was 650°K compared to the experimental value of 400°K. The calculated value for OEL was 560° compared to the experimental value of 480°K.

superimposed on the curve of T vs I obtained experimentally for OMPL. A scaling factor was used to set the maximum of the calculated curve to the maximum of the experimental curve in order to compare the curve shapes. The figure illustrates that there is a good fit between the calculated and experimental curves.

Figure 23 shows a plot of magnet current versus time and  $\int I^2 dt$  versus time after a heater-induced quench is started at OEL at 33.3 millisecc. The time constant for the current decay from its initial constant value is about 267.5 millisecc. The bump in the current decay curve is caused by the interaction of the two power supplies.

The comparisons of calculated with experimental results indicate that the functional dependences of  $T_m$ ,  $v_q$  and  $v_a$  on  $I_q$  and I as given by the several formulas are not unreasonable. The curves of Fig. 17 plotting the temperatures of OEL and OMPL versus current are not inconsistent with those of Figs. 5 and 6. For a current of 5.0 kA, for example, the temperature at OEL is higher than that at OMPL while the longitudinal quench velocity at OEL (Fig. 6, 4-8) is lower than at OMPL (Fig. 5, 4-8).

The calculated values for  $T_m$  at 4.5 kA and 4.5°K at OEL and OMPL are significantly higher than the measured values. This difference is not unexpected since the relationship used to calculate  $T_m$  uses rather conservative assumptions, i.e., no cooling from the helium.

G. Cottingham, using these experimental results and information from G. Morgan, has calculated that a single diode passive quench protection system for the SSC magnet in TN-23 will give a margin of safety of about 1.0 MIITS while a double diode passive system will increase the margin of safety to almost 3.0 MIITS.

One further comment. It should be pointed out that the curves of velocity versus current should intersect the abscissa at some low value of current, not

References

1. P. Dahl et al., "Performance of Four 4.5 m Two-in-One Superconducting R&D Dipoles for the SSC," these proceedings.
2. G. Ganetis and A. Stevens, "Results of Quench Protection Experiment on DMI-031," SSC Technical Note No. 12, Brookhaven National Laboratory.

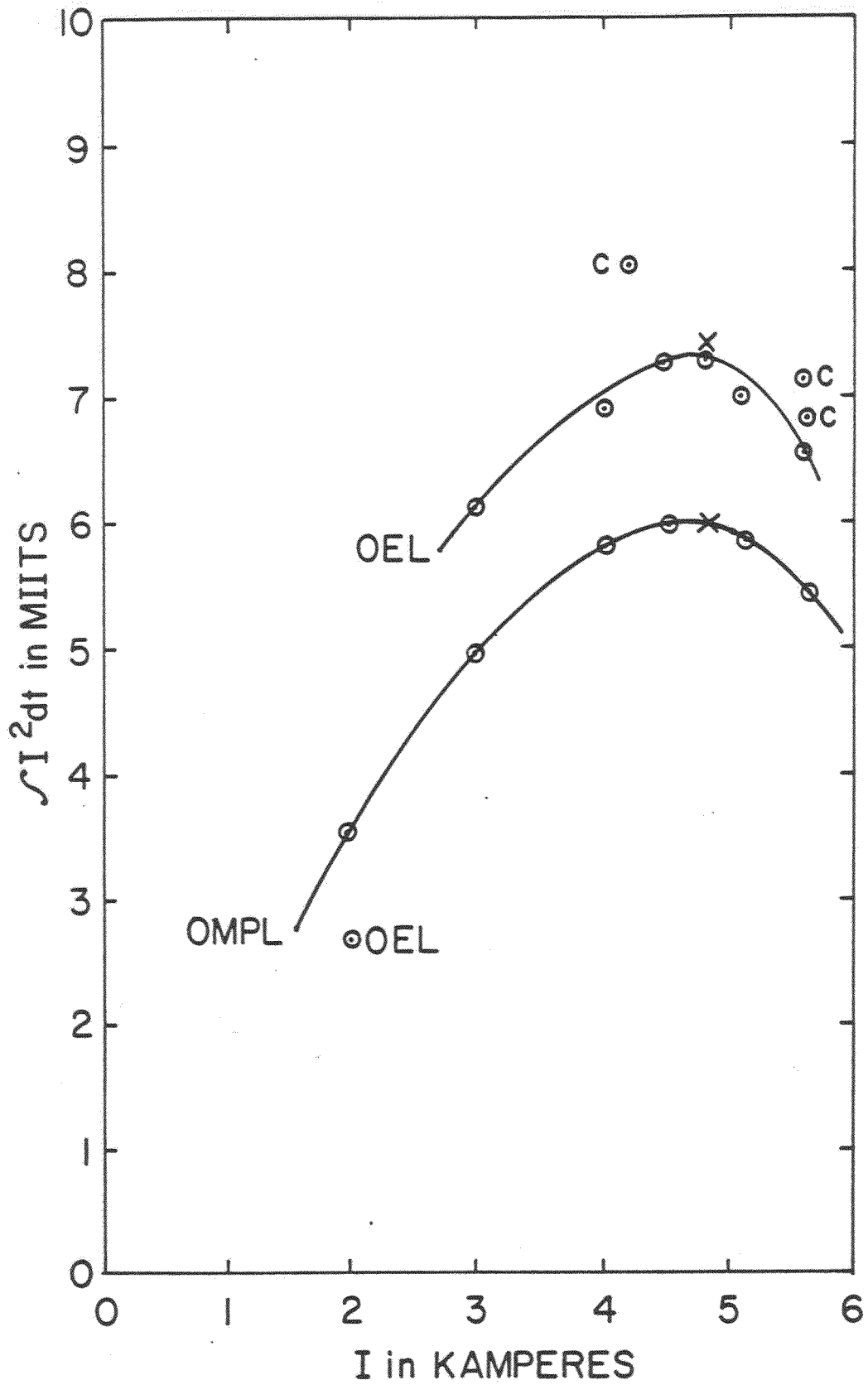


Figure 2.  $\int I^2 dt$  vs  $I$  for Outer Coil at  $4.4^\circ K$ .

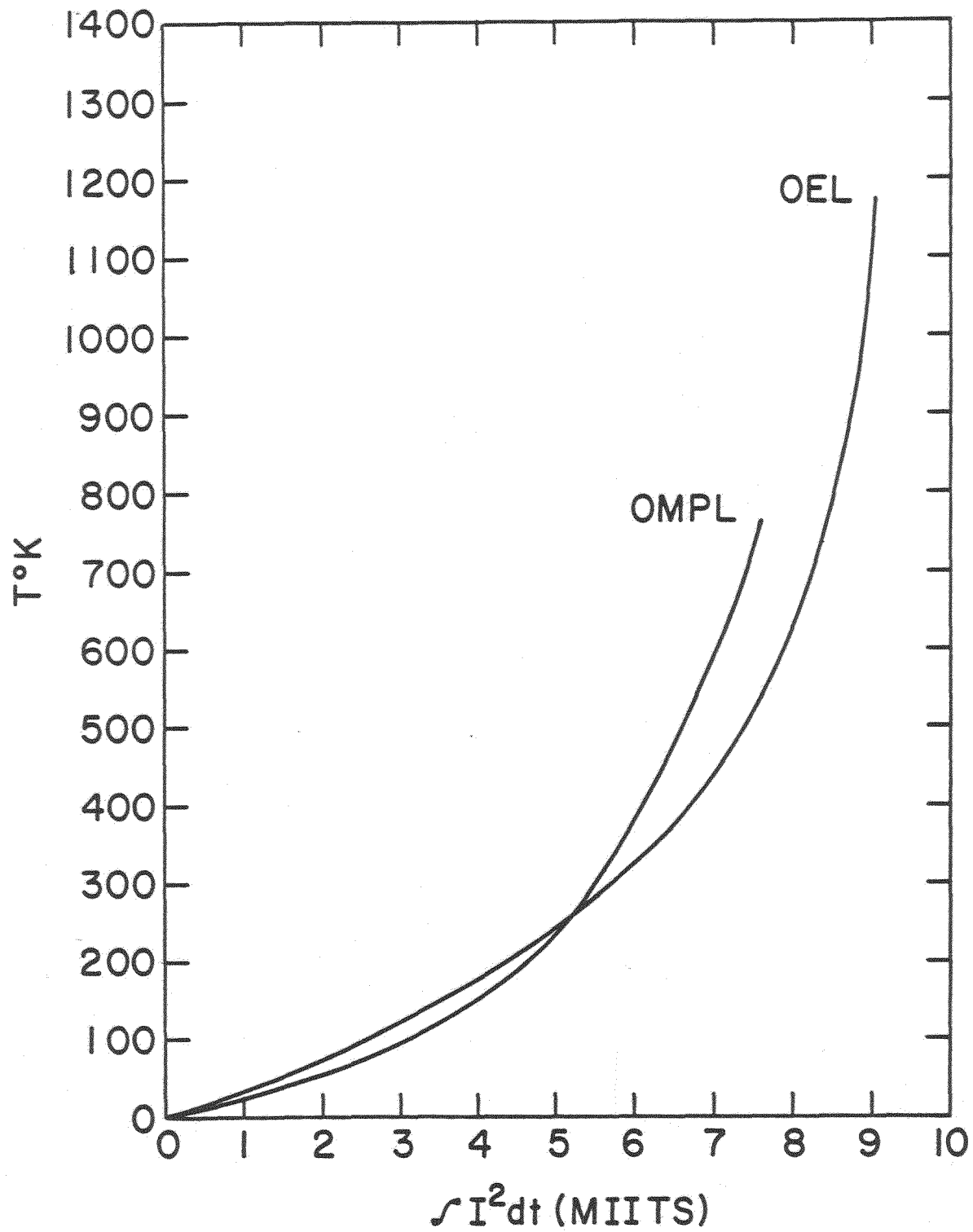


Figure 4. T vs  $\int I^2 dt$  for OMPL and OEL.

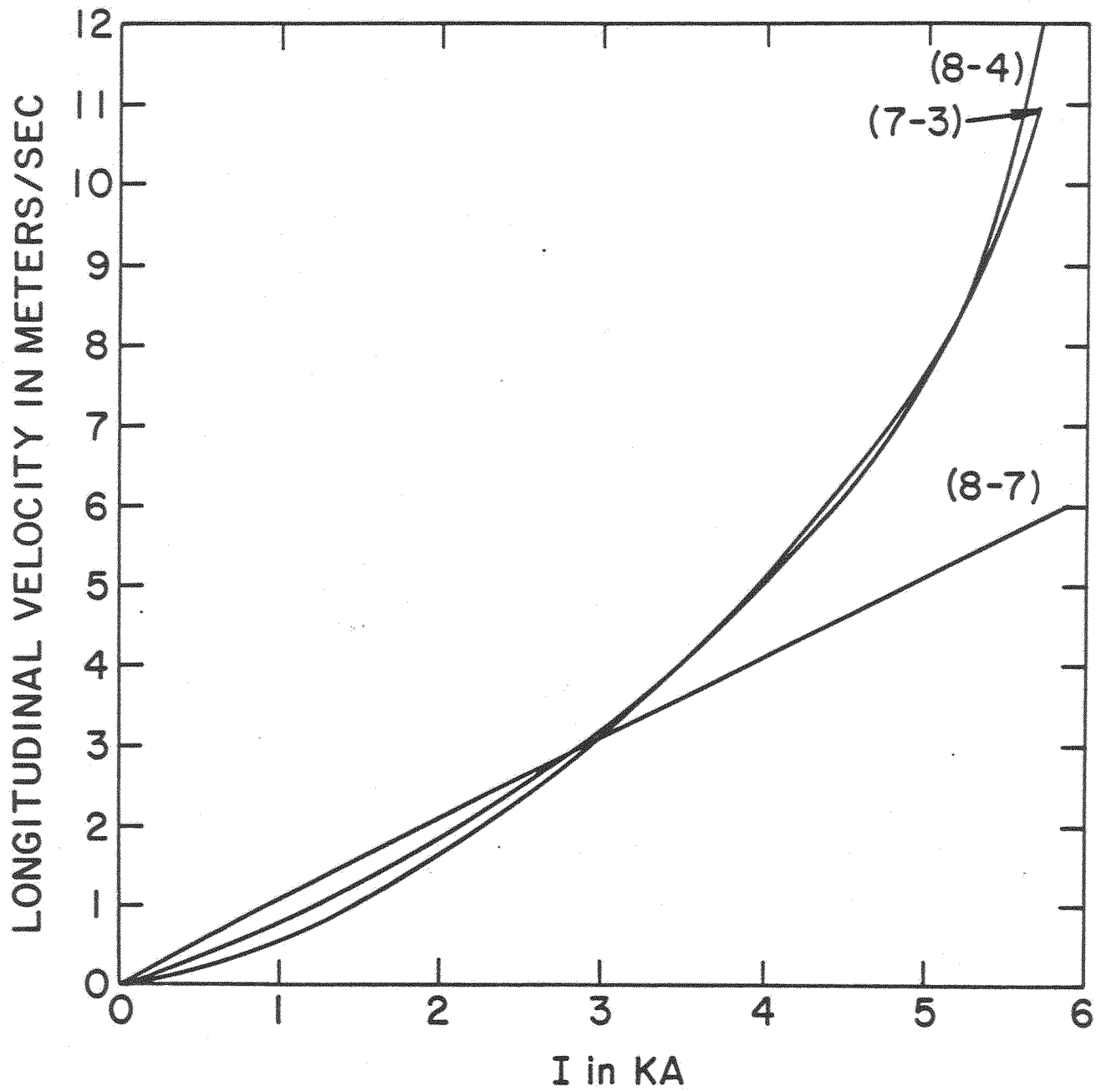


Figure 6. OEL: Longitudinal Quench Velocity vs I at 4.5°K.

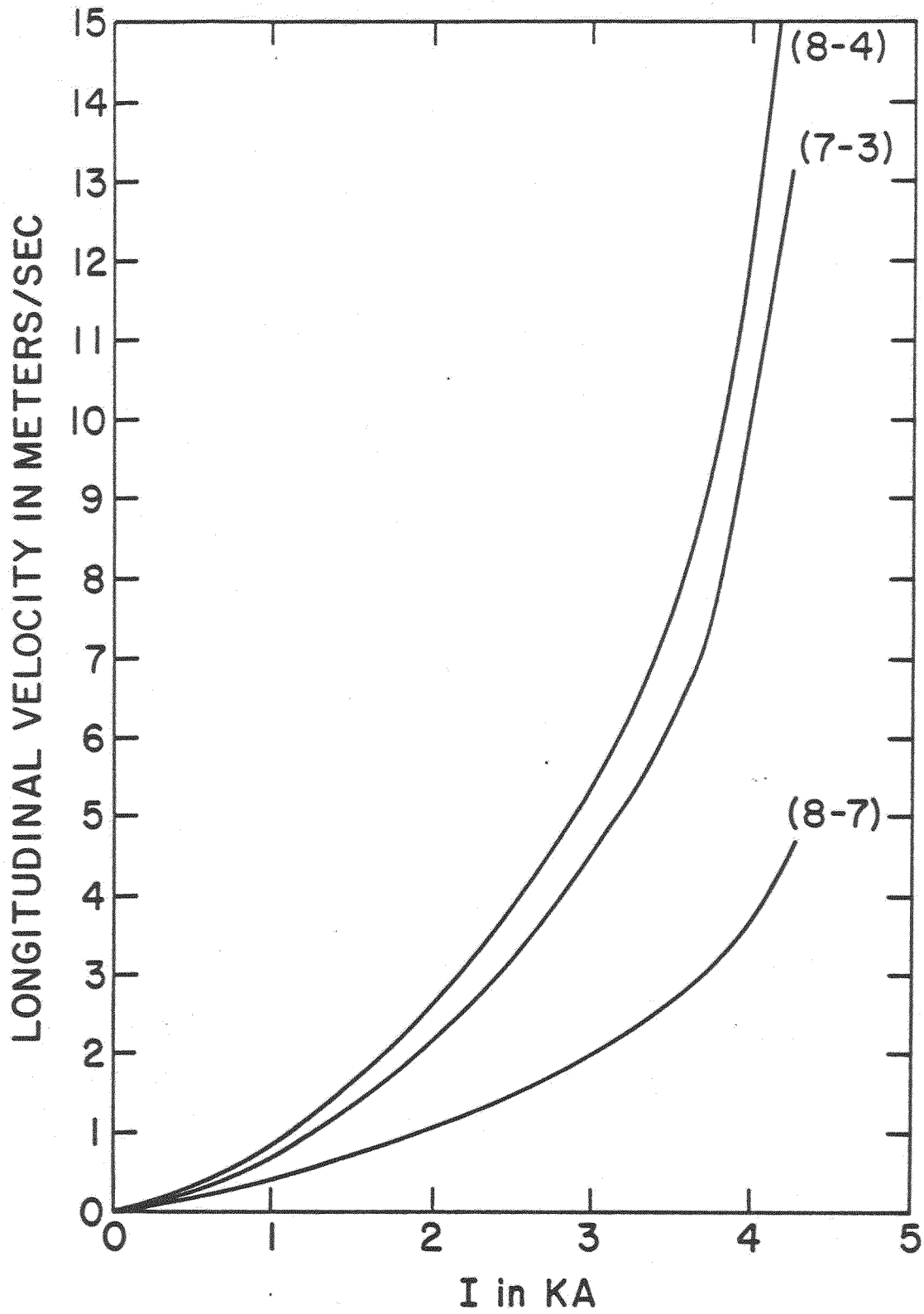
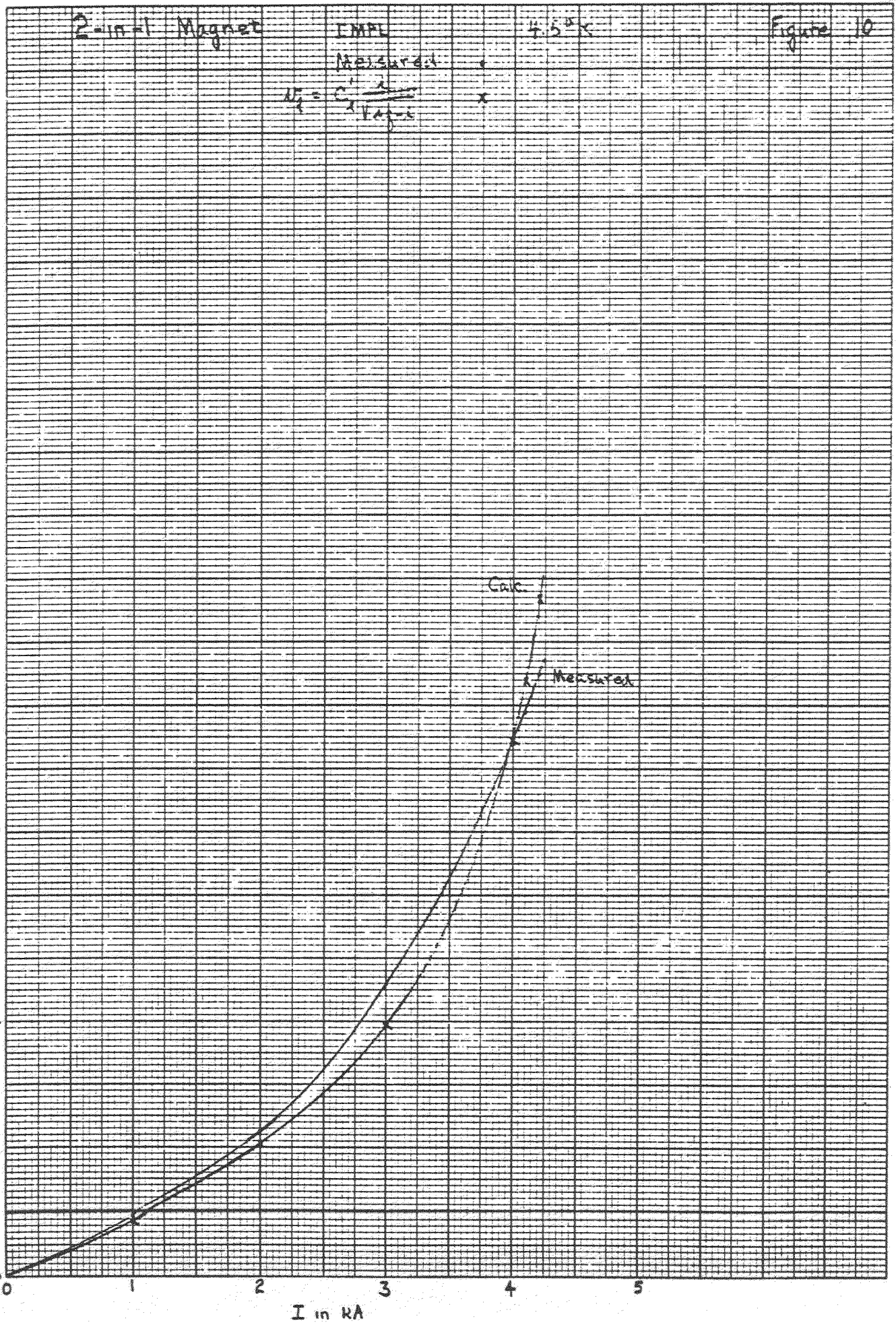


Figure 8. IEL: Longitudinal Quench Velocity vs I at  $4.5^{\circ}\text{K}$ .

Longitudinal Velocity in Meters/Sec



Azimuthal Velocity in Meters/sec

0.06  
0.05  
0.04  
0.03  
0.02  
0.01  
0.0

2-in-1 Magnet

INPL

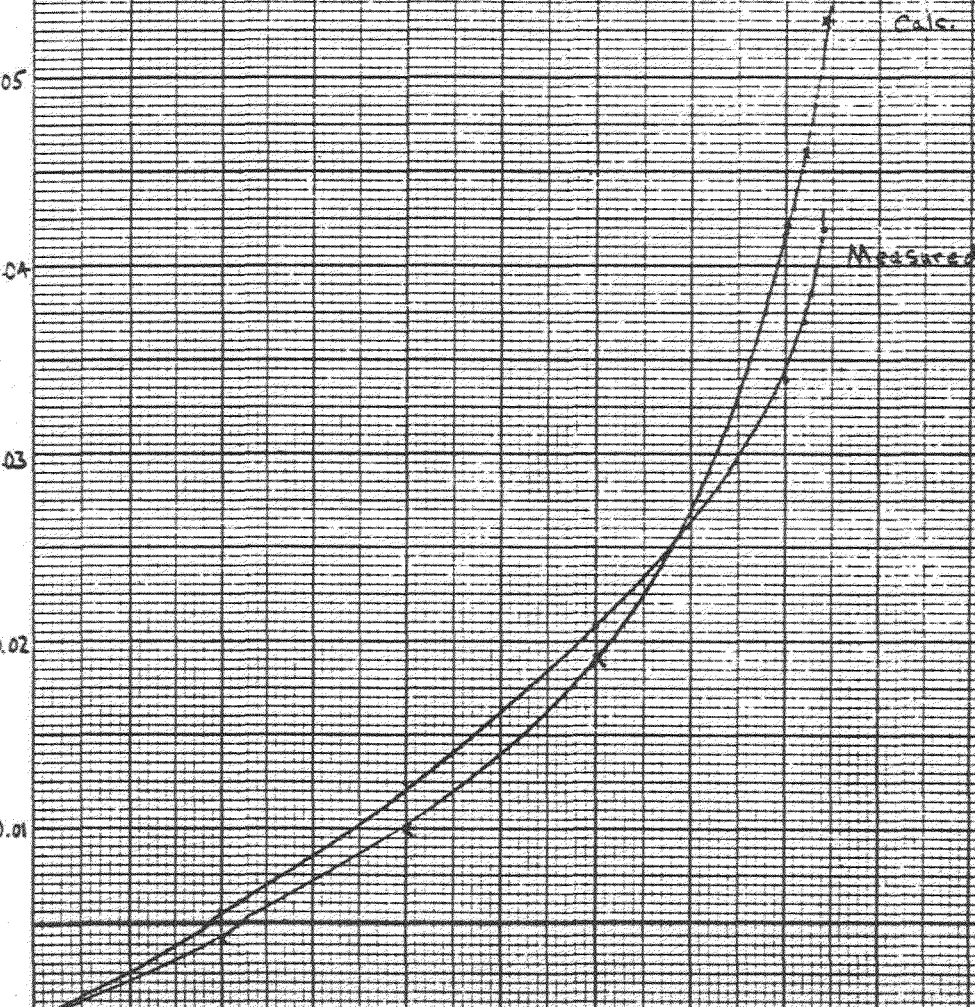
4.5°K

Figure 12

Measured

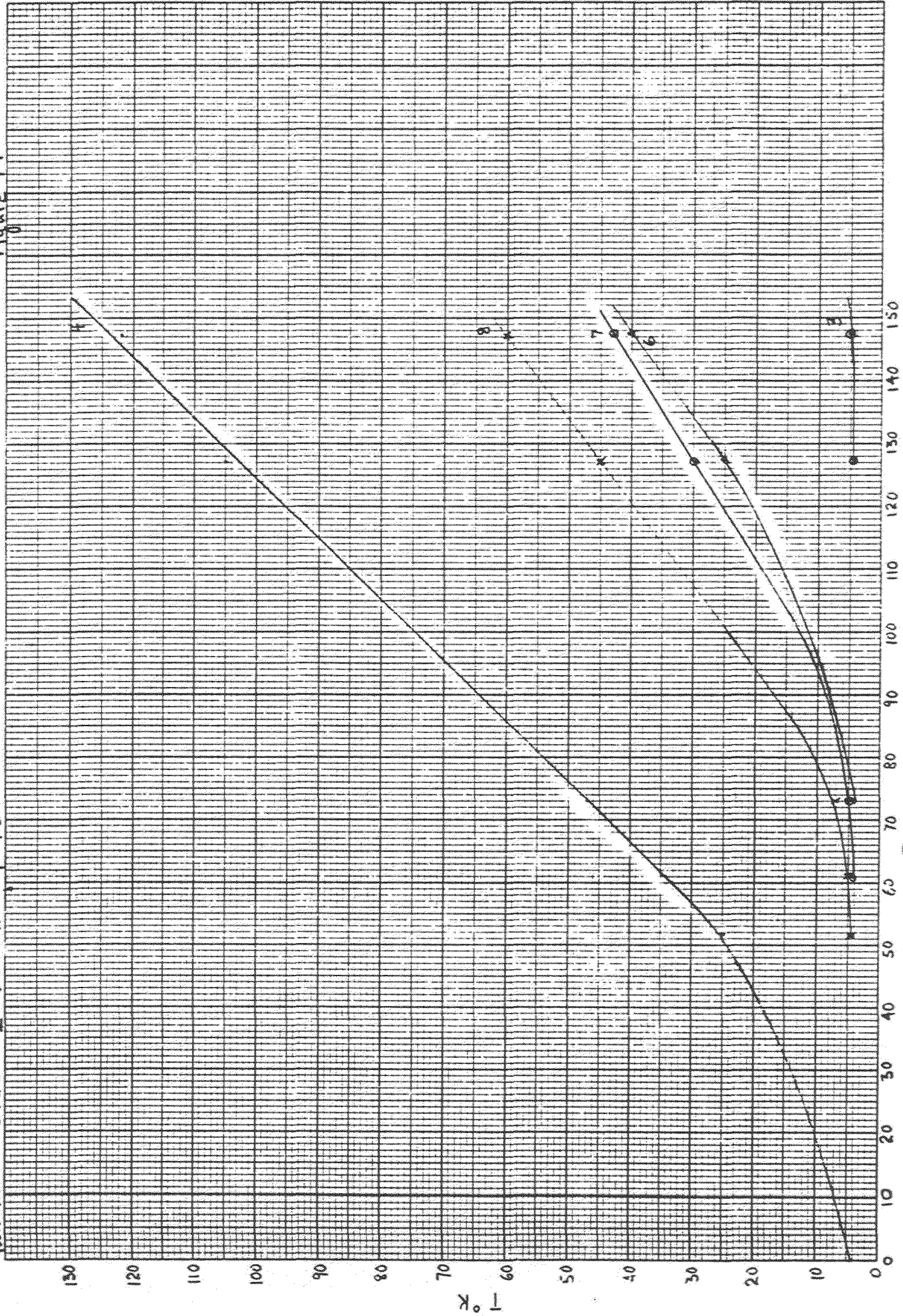
$$V_a = \frac{r \cdot \omega}{r_{in}}$$

0 1 2 3 4 5  
I in KA



File 103 - 0 MPL - I = 4.802 AA T = 4.5 K

Figure 14



File 167-OEL, I = 5.6 kA, T = 2.8-26 K

Figure 16

OEL 2-in-1 Magnet

GRAPHIC CONTROLS CORPORATION  
10 X 10 TO THE HALF INCH AS 0813 CU

GRAPHIC CONTROLS CORPORATION  
Huntington, New York Printed in U.S.A.

GRAPH PAPER

T °K

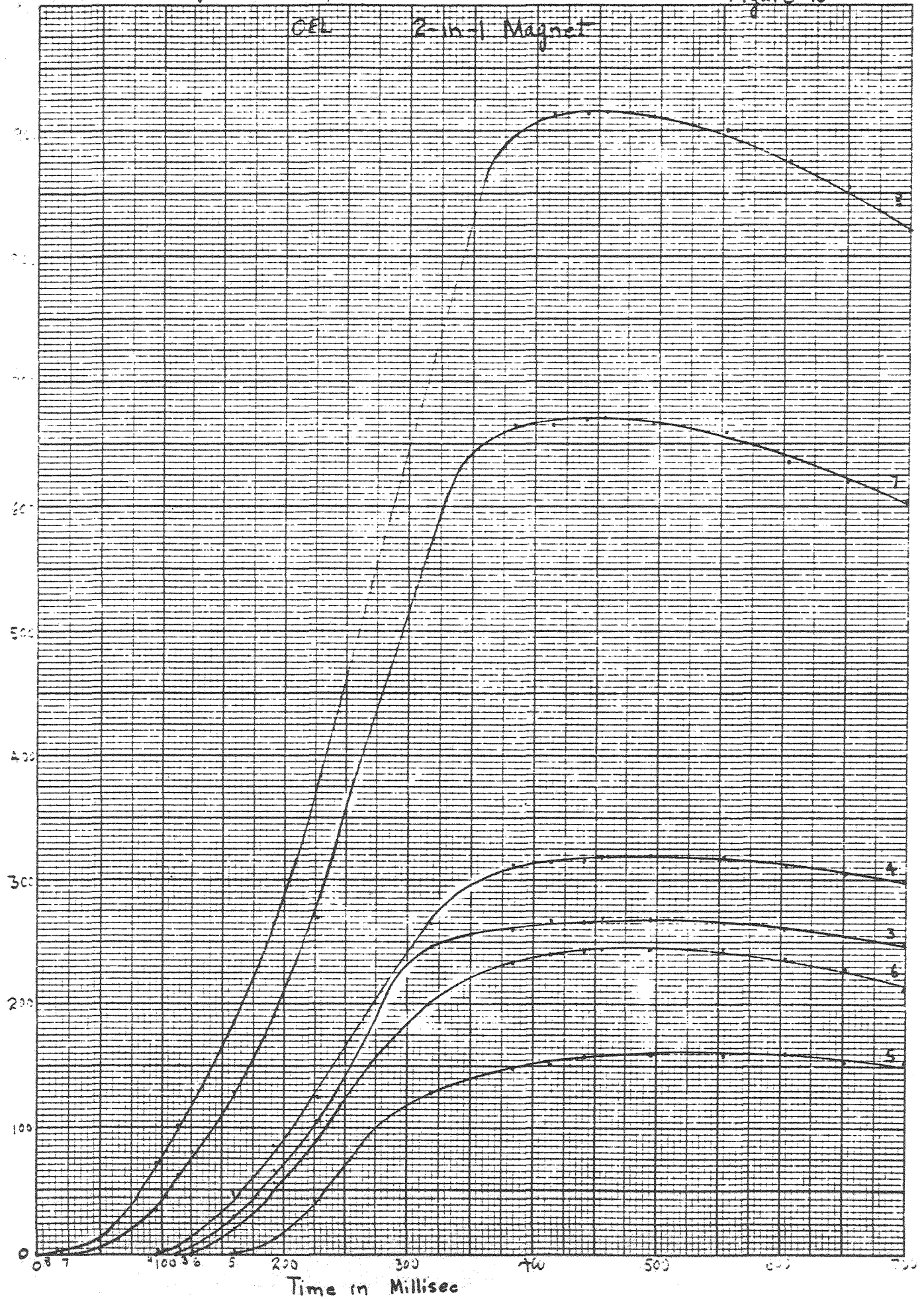
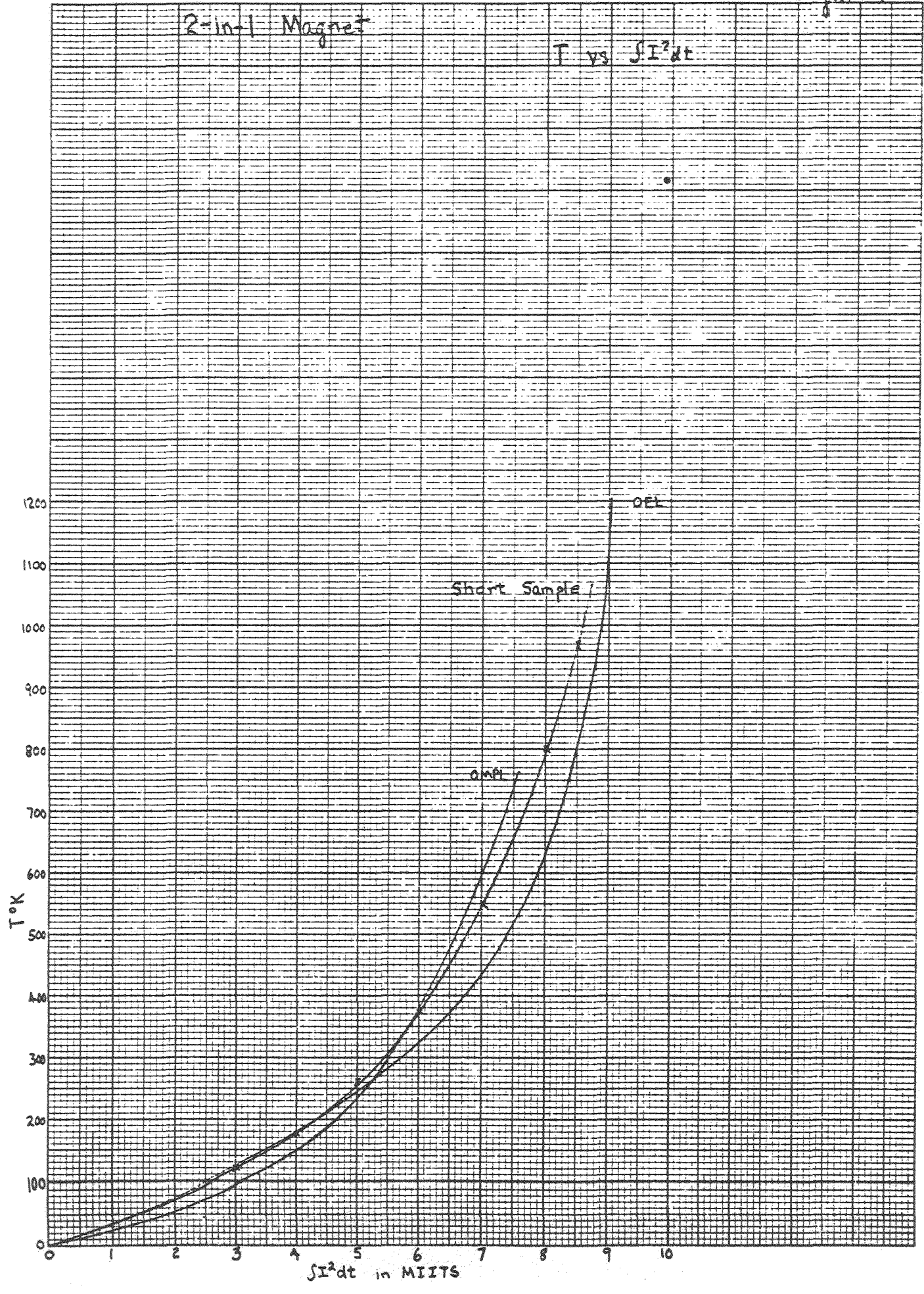


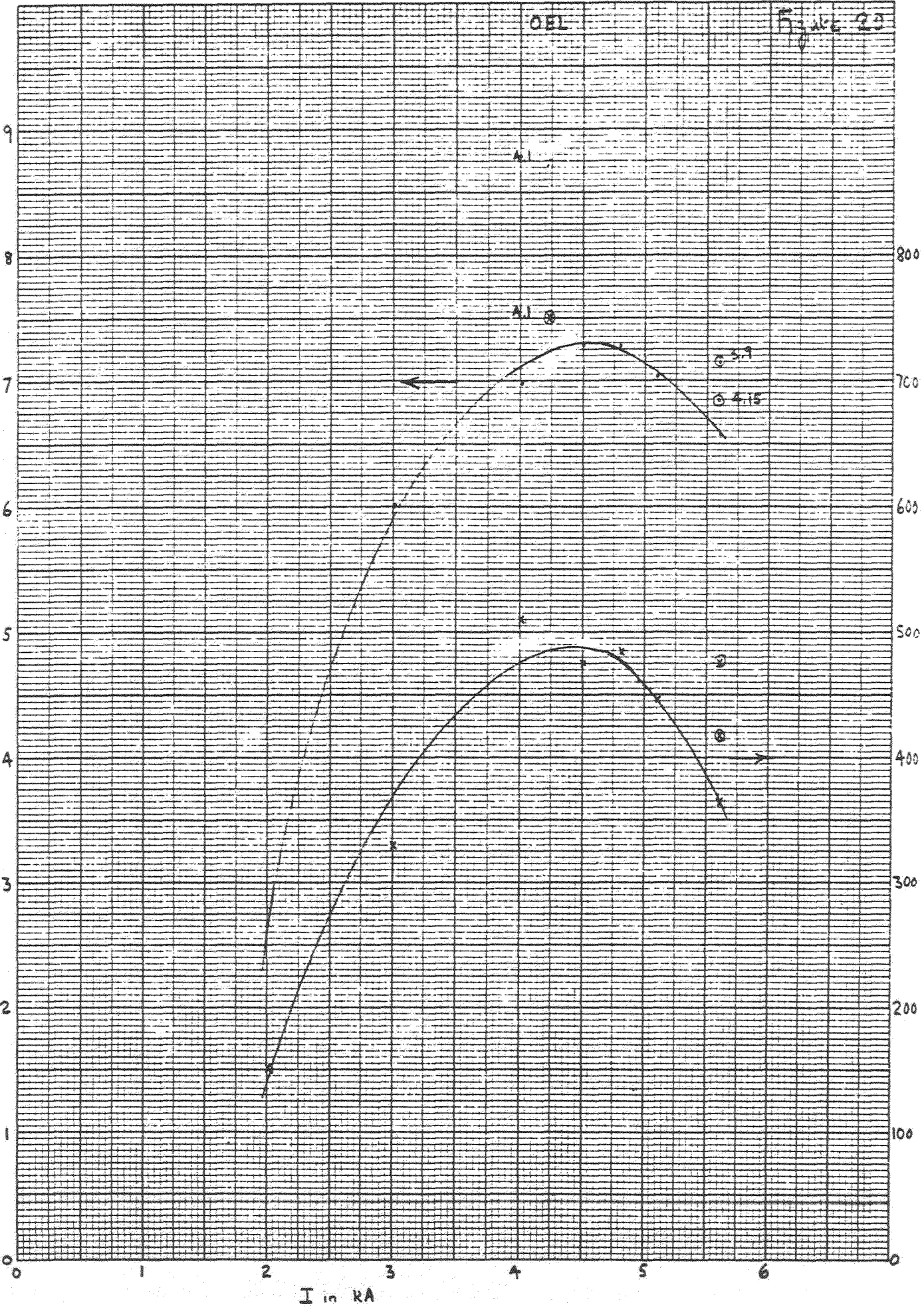
Figure 13

2-in-1 Magnet

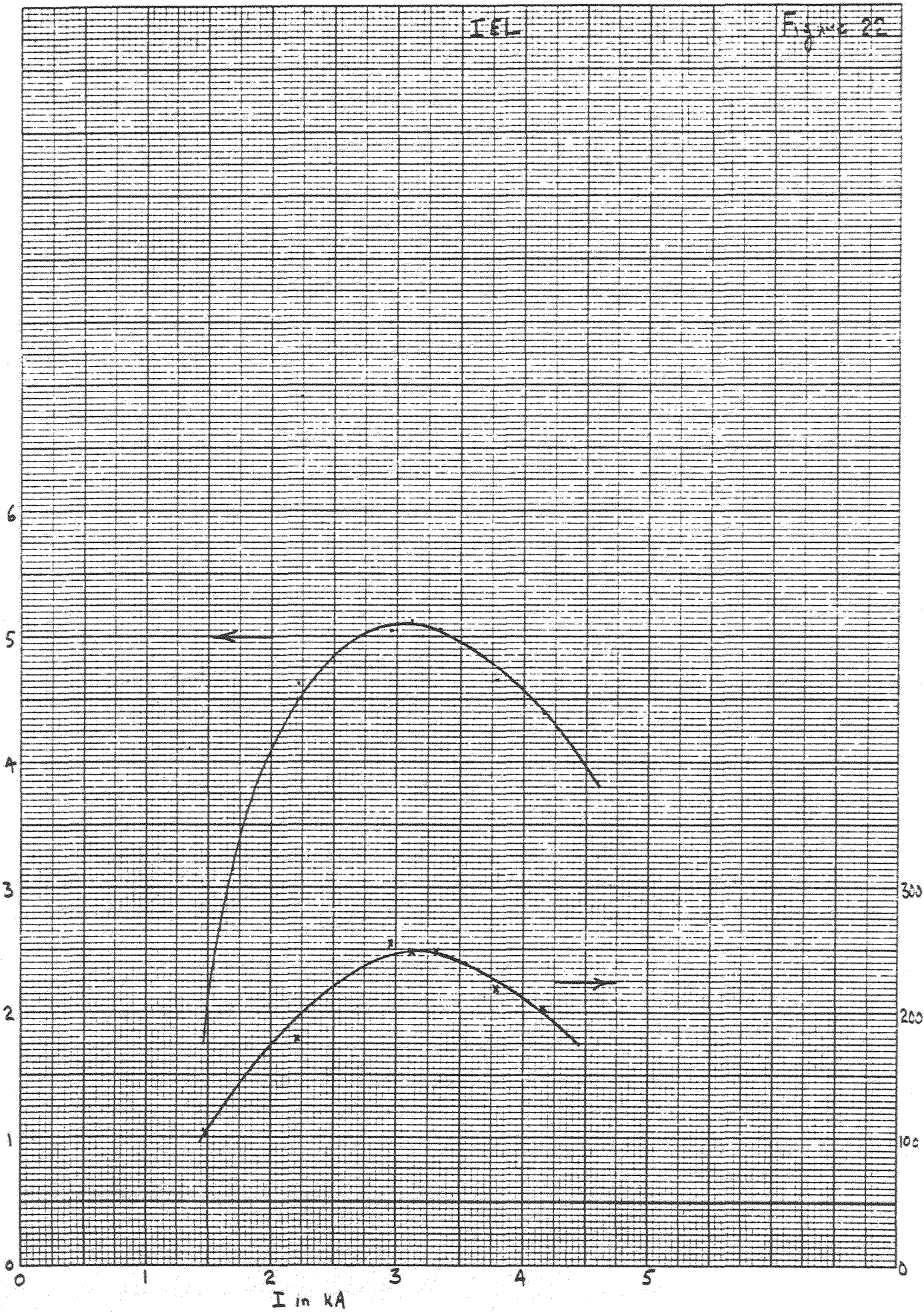
$T$  vs  $\int I^2 dt$



$\int I^2 dt$  in MIITS



$\int I^2 dt$  in MIIIS



IEL

Figure 22

300  
200  
100

K

Revised 8/29/85

DISTRIBUTION

BLDG. 911

AD Library  
(H. Martin)  
G. Bunce  
H. Foelsche  
J. Grisoli  
P. Hughes (1) + 1  
for each author  
D. Lazarus  
D. Lowenstein  
T. Sluyters

FOR SSC PAPERS

FNAL

C. Rode  
W. Fowler

LBL

R. Donaldson (2 copies)  
P. Limon  
C. Taylor  
M. Tigner  
R. Wolgast

BLDG. 902

D. Brown  
J. Claus  
J.G. Cottingham  
E. Courant  
P. Dahl  
F. Dell  
A. Flood  
M. Garber  
C. Goodzeit  
A. Greene  
R. Gupta  
H. Hahn  
H. Halama  
K. Jellett  
E. Kelly  
S.Y. Lee  
R. Louttit  
G. Parzen  
A. Prodehl  
P. Reardon  
W. Sampson  
R. Shutt  
J. Sondericker  
S. Tepekian  
P. Wanderer  
E. Willen

BLDG. 460

N. Samios

BLDG. 510

H. Gordon  
T. Kycia  
L. Leipuner  
S. Lindenbaum  
R. Palmer  
M. Sakitt  
M. Tannenbaum  
L. Trueman  
D. White

BLDG. 535

W. Casey

BLDG. 725

M. Barton

S&P in Magnet Division for all MD papers

S&P in Cryogenic Division for all Cryo Papers  
(and J. Briggs, R. Dagradi, H. Hildebrand  
W. Kollmer)